Influence of Polymer Characteristics and Melt-Spinning Conditions on the Production of Fine Denier Poly(Ethylene Terephtalate) Fibers. Part I. Rheological Characterization of PET Polymer Melt

CHANG T. KIANG* and JOHN A. CUCULO†

North Carolina State University, Fiber and Polymer Science, Raleigh, North Carolina 27695-8302

SYNOPSIS

The rheological characterization of four poly(ethylene terephtalate) (PET) polymers, with viscosity average molecular weight ranging from 2.7×10^4 to 7.1×10^4, has been performed in the Instron capillary rheometer. The apparent elongational viscosity was obtained from the shear flow and entrance pressure data, following the methods proposed by Cogswell and Binding in contraction flow experiments. The PET polymers showed a tension thinning behavior in the deformation rate range of 300–3000 s^{-1} employed in this study. These results were explained on the basis of the network model. Polymers with similar behavior in shear may be distinct in elongational and may lead to distinct polymer processability. Polymers with lower apparent elongational viscosity level were shown to allow spinning of finer denier fibers, which is determined by the polymer spinnability.

INTRODUCTION

The ultimate objective of this research is the study of the formation mechanism of fine denier poly(ethylene terephtalate) (PET) fibers in the high-speed melt-spinning processes. The motivation of this research comes from both the growing economic interest associated with the high-value products that result from the unique properties of the fine denier fibers and from the scientific challenges of determining the parameters that influence the limiting fineness of the fiber. The lower limit of the as-spun fiber denier can be associated with the limit of the polymer spinnability, which depends on the melt spinning conditions as well as on the rheological properties of the polymer melt.

The rheological properties of polymer melts can be determined in either shear or elongational flow. Most of the data presented in the literature are determined in shear flow experiments, e.g., in rotary or capillary extrusion experiments. In the melt-spinning process the shear viscosity is important to describe the flow of the polymer melt up to its exit from the capillary of the spinneret, such as in determining the power consumption of the extruder, the pressure drop in the filtration media and in the capillaries of the spinneret.

However, the attenuation of the extrudate is determined by an elongational flow in the region between the spinneret and the solidification point of the threadline. The elongational viscosity of the polymer therefore determines the stress level in this region of the threadline, and, consequently, it is expected to be important in the results of the minimum denier attainable during melt-spinning processes.

There has been an increasing number of studies on the elongational behavior of polymers, but they have been unable to circumvent the difficulties of obtaining a steady-state value of stress in a constant strain rate experiment, especially at higher strain rates (ca. 1 s^{-1}). Moreover, in the nonisothermal spinning process, the strain rate as well as the temperature vary along the threadline.

The apparent elongational viscosity obtained via contraction flow experiments, following the methods

* Present address: Rhodia S.A., Sao Paulo, S.P., Brazil.
† To whom correspondence should be addressed.

Journal of Applied Polymer Science, Vol. 46, 55–65 (1992)
 CCC 0021-8995/92/010055-11$04.00

of Cogswell[1] and Binding and Walters,[2,3] seems to be particularly attractive to characterize different PET polymers in the range of strain rate experienced by the threadline. The elongational viscosity determined in this experiment should be interpreted only as an apparent value because the strain rate changes along the contraction.

Since the strain rate is also variable in the actual spinning process, it seems possible to relate elongational viscosity characteristics determined in contraction flow experiments to the melt-spinning behavior.

EXPERIMENTAL

Materials

Four types of linear PET [poly(ethylene terephtalate)] were employed in this study. The intrinsic viscosity (IV) of the polymer chips was measured as-received in phenol/1,1,2,2-tetrachloroethane (60/40) at 25°C in Ubbelohde type viscometers. The viscosity average molecular weight, M_v, was calculated from the Mark–Houwink equation $IV = KM_v^a$ where the coefficients K and a were 7.44×10^{-4} dl/g and 0.648, respectively.[4] These results are summarized in Table I.

Capillary Rheometry

The shear viscosity curves were obtained in an Instron Capillary Rheometer (ICR) with capillary diameter $D = 0.030$ in. and length $L = 1.000$ in. ($L/D = 33.3$). The polymer chips were dried in a vacuum oven at 140°C for 12 h prior to the extrusion experiments. The extrusion temperature was 280°C.

The thermal stability of the PET polymers were evaluated from the recorded pressure drop data during 2 h of extrusion in the ICR at 280°C with the capillary 0.030×1.000 in. at constant shear rate ($69.4\ s^{-1}$).

The entrance pressure data may be obtained following the methodology proposed by Bagley,[5] using a series of capillaries of the same diameter but different lengths. A plot of the pressure drop versus L/D is linear, and the entrance pressure P_0 is obtained by the intercept at $L/D = 0$. Four capillaries were used for the experiments in the ICR, with diameter of 0.030 in. and length of 0.110 in. ($L/D = 3.67$), 0.240 in. ($L/D = 8$), 0.480 in. ($L/D = 16$), and 1.000 in. ($L/D = 33.33$).

An alternative method is the direct measurement of P_0 with a knife-edge die ($L = 0$).[6] The knife-edge die employed in this study has a diameter equal to 0.014 in. and a flat entry. The measurements were conducted at a temperature of 280°C.

Table I Characterization of the PET Samples

Sample	Supplier	IV	M_v
A	Goodyear	0.56	27,493
B	Rhone Poulenc A	0.64	33,784
C	Celanese	0.66	35,427
D	Goodyear	1.04	71,467

Elongational Flow Behavior

The shear flow data and the entrance pressure data were used to calculate the apparent elongational viscosity parameters, following the method originally proposed by Cogswell,[1] as well as the more recent method proposed by Binding.[2] For simplicity, the term *apparent elongational viscosity* will be implicit when referred to as elongational viscosity throughout this work.

In the Cogswell analysis the following equations were derived to calculate the extensional stress σ_E and extensional rate ϵ_E:

$$\sigma_E = \frac{3(n+1)P_0}{8} \tag{1}$$

$$\epsilon_E = \frac{4\mu_s \epsilon_{s_0}^2}{3(n+1)P_0} \tag{2}$$

where P_0 is the entrance pressure drop measured at the wall, ϵ_{S_0} is the wall shear rate at the entrance of the capillary, μ_S is the shear viscosity, and n is the shear flow behavior index.

The Binding analysis starts with the assumption of a power law model for both shear and elongational flow that is then related to the entrance pressure drop. If K, n are the consistency and flow behavior index in shear flow and L, t are the consistency and flow behavior index in elongational flow, the following results:

$$P_0 = \frac{2K(1+t)^2}{3t^2(1+n)^2}\left(\frac{Lt(3n+1)n^t I_{nt}}{K}\right)^{1/(1+t)} \times (\epsilon_s)_{R0}^{t(1+n)/(1+t)}(1 - \alpha^{3t(1+n)/(1+t)}) \tag{3}$$

where

$$\text{Int} = \int_0^1 \text{abs}\left[2 - \frac{3n+1}{n}\phi^{1+1/n}\right]^{t+1} \phi\, d\phi$$

and $\alpha = R_0/R_1$, R_0 is the radius of the capillary and R_1 is the radius of the ICR barrel.

Flow Visualization

The apparatus used for the flow visualization experiments is the same used by Crater,[7] except for modifications in the way the die housing assembly is attached to the spin block and extruder. The quartz dies, 2 in. diameter and 1 in. thick, were used to prepare transparent capillary dies with flat entrance, where the dimensions of the upstream reservoir was 0.374 in. diameter and 0.7 in. long, and the downstream capillary diameter was 0.04 in. and length was 0.3 in. As opposed to the ultrasonic impact grinder used formerly to prepare the dies, a drilling process was used to prepare the dies in the present study. A diamond compound, grade 16 to 1 μm, was used to polish the reservoir walls to achieve transparency.

The illumination system was similar to the one used in Crater's experiments and consisted of a 0.5-mW helium–neon laser and four semicylindrical lens that focused the laser beam into a narrow slit of approximately 2 in. wide. Streak photography was performed using a Canon F-1 35-mm camera and a Canon FD50 mm f/3.5 SSC macro lens adapted with a FD25 extension tube, which produced an object to image ratio of 1 : 1. Exposure times ranging from 30 s to 2 min were used with Kodak Tmax 400 film.

Aluminium particles, 50–150 μm diameter, were thoroughly mixed with the polymer prior to drying at a concentration of 50 ppm.

RESULTS AND DISCUSSIONS

The shear flow curves of the four polymer samples are shown in Figure 1. It can be seen that polymers A and D, which correspond to the minimum and maximum value of IV among the four samples, correspond to the extremes of shear viscosities in the interval of shear rate employed in this study. Polymers B and C have intermediate shear viscosities. Furthermore their shear viscosities are not distinguishable in the shear rate range studied, despite the slight differences in their IV. We can also observe that for all four samples, newtonian behavior can be expected at shear rate lower than 10^2 s^{-1}.

The results in Figure 2 indicate that polymer A shows the greatest viscosity retention after 2 h of extrusion at 280°C whereas the high-viscosity polymer, D, has the largest viscosity drop. Polymers B and C present intermediate results, however, closer to the low IV polymer A. The greater viscosity retention makes polymers of lower IV, in particular polymer A, more suitable, from the standpoint of thermal stability, for the fine denier process due to the usually lower throughputs and consequently higher residence time involved in these processes.

The pressure drop at the entrance of a capillary has been traditionally associated with the visco-

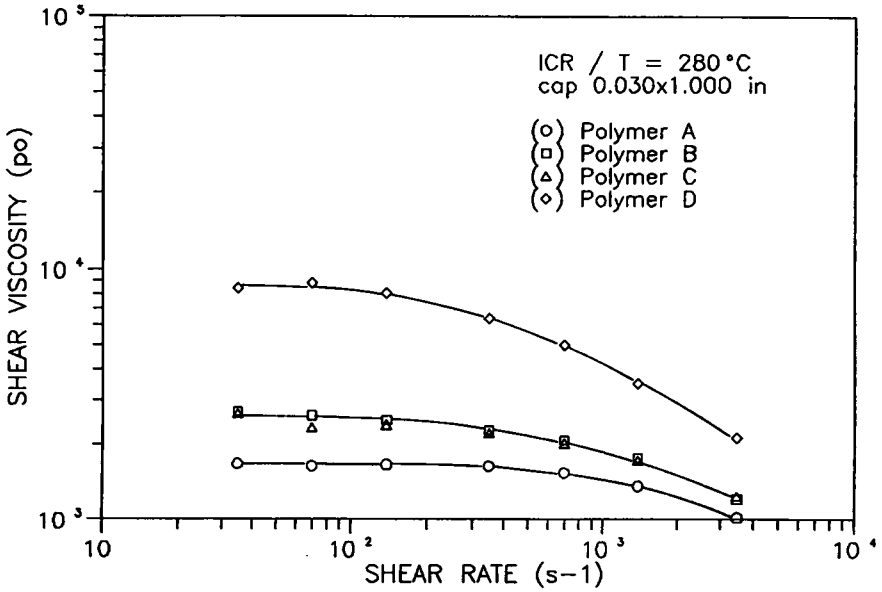

Figure 1 Shear flow curve; temperature = 280°C. Instron capillary rheometer, cap. 0.030 × 1.000 in.

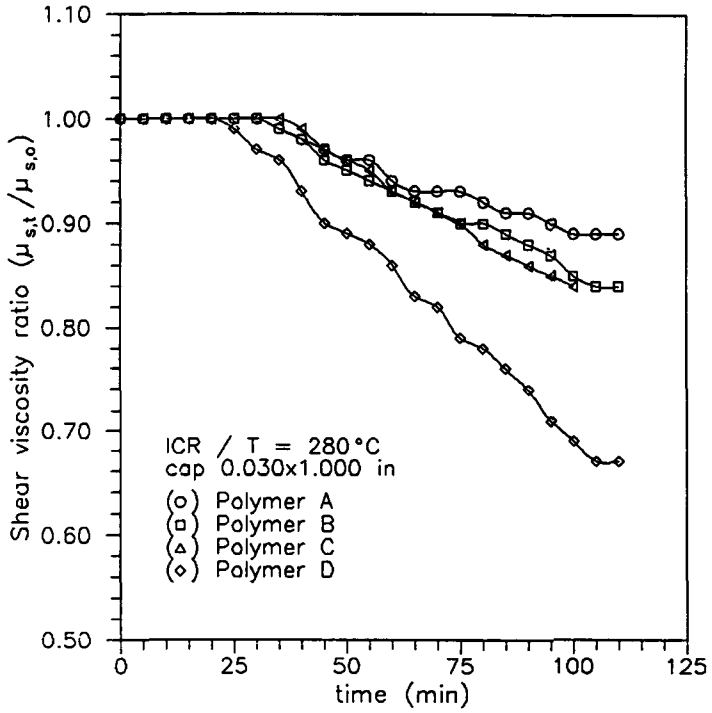

Figure 2 Thermal stability of PET polymers at 280°C. Fraction of initial shear viscosity at the shear rate of 69.4 s^{-1} versus extrusion time.

elastic effects due to the sudden change of velocity profile in this region. Its value has been used as a measure of the first normal stress difference[8] or in the determination of the shear modulus[9] by plotting the entrance correction from Bagley's analysis versus the shear stress. The shear modulus is then given by $(2 \times \text{slope})^{-1}$. The shear modulus for polymers A and D were obtained by this method and shown in Figure 3. The values obtained for the two polymers may be considered the same and approximately equal to 2×10^6 dyn/cm^2.

The results of the entrance pressure drop obtained with the Bagley's plot were compared with those obtained with the knife-edge die and shown in Figure 4. It can be seen that both methods lead to similar results, except that the linearity of the plots of log P_0 versus log shear rate is better with the knife-edge die. Both methods are limited to shear rates larger than 300 s^{-1} due to the sensitivity of the pressure readings in the Instron capillary rheometer.

Figure 5 shows the results of entrance pressure obtained from knife-edge die at the temperature of 280°C. These results show that the entrance pressure is larger the larger the shear viscosity. In addition the entrance pressure at a given shear rate for polymer B is larger than for polymer C while the shear viscosities are similar.

Figure 6 presents the results of elongational viscosity at 280°C, obtained from Binding's method. Figure 7 gives the corresponding results using Cogswell's method. It can be seen that both methods present the same qualitative results, but the results from Cogswell's analysis have consistently higher magnitudes.

These results indicate that the elongational viscosity decreases with increase in elongational rate for all polymers in the range of deformation rate of 300–3000 s^{-1}. The higher IV polymers tend to present higher values of elongational viscosity, except for samples B and C. Sample B, despite its slightly lower IV than sample C but with similar shear viscosities, shows larger elongational viscosity than sample C.

The flow visualization experiments indicated no vortex enhancement with increase in shear rate, as shown in Figures 8 and 9 for polymers A and B, respectively. The vortex detachment length for polymers A and B is approximately equal to the radius of the upstream reservoir.

Interpretation of the Apparent Elongational Viscosity Data Obtained in Contraction Flow

There are not enough data in the literature on the elongational viscosity behavior of PET melts. The results by Hill and Cuculo[10] show a tension thick-

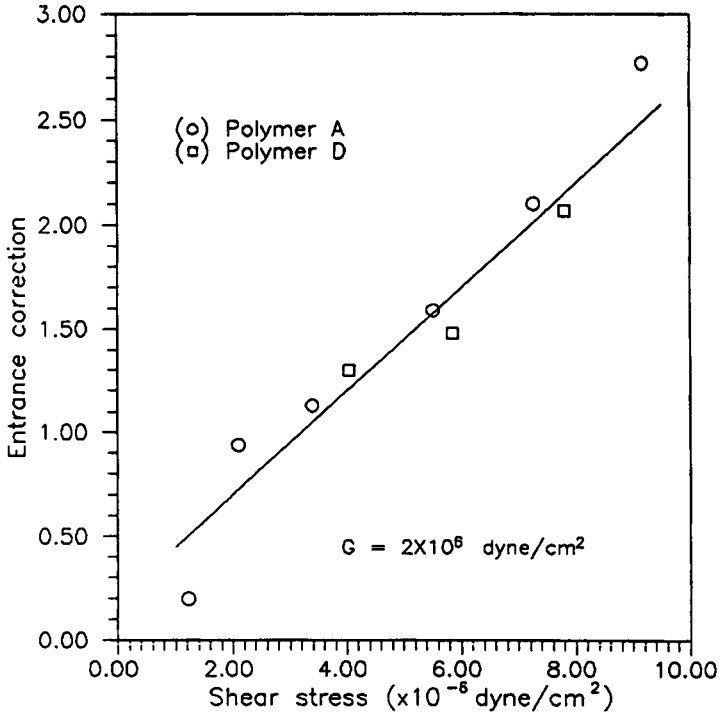

Figure 3 Separation of elastic and viscous effects from entrance correction determined by Bagley's plot at 280°C (G = shear modulus).

ening behavior; however, the elongational rates employed were lower than 6 s^{-1}. In a collaborative study of the rheological properties of PET polymers,[11] the elongational viscosity of the linear polymers were reported to decrease with an increase in the shear stress whereas branched polymers showed an in-

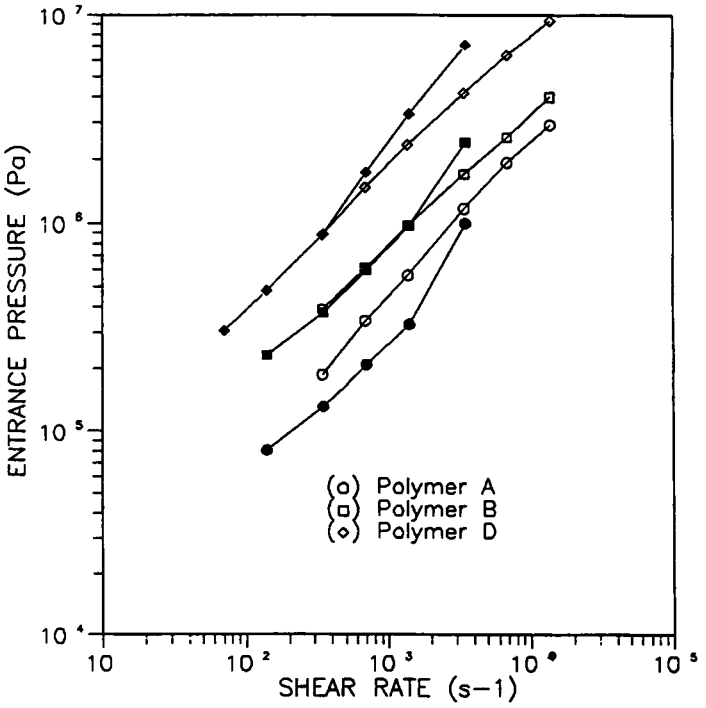

Figure 4 Entrance pressure of PET polymers at 280°C determined from knife-edge die D = 0.014 in. (unfilled symbols) and Bagley's plot D = 0.030 in. (filled symbols).

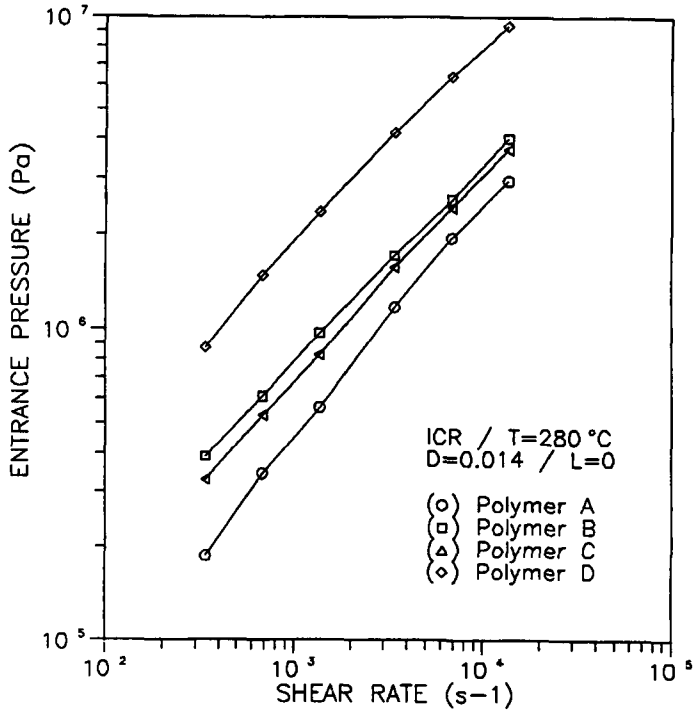

Figure 5 Entrance pressure of PET polymers at 280°C determined from knife-edge die $D = 0.014$ in.

crease of elongational viscosity with an increase in shear stress. The results were obtained at 285°C using Cogswell's entrance flow technique, in the shear rate range near 10^3 s^{-1}. It is speculated that the elongational viscosity behavior of polymers may go through a maximum as a function of the elongational rate,[6] with the Trouton viscosity at the limit of zero elongational rate, tension thickening at low elongational rates, and tension thinning at higher elongational rates.

These results can be qualitatively explained using a network model[12] made up of temporary junctions,

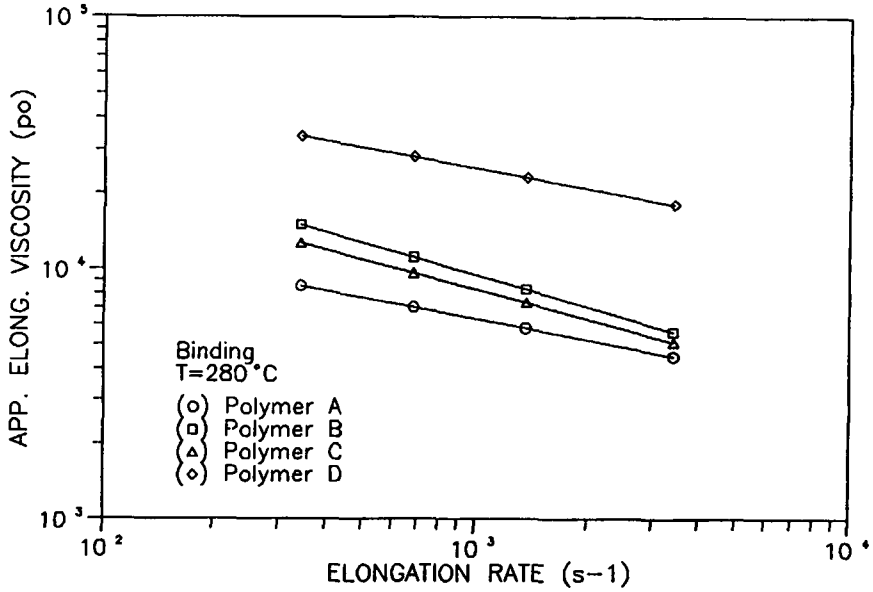

Figure 6 Apparent elongation viscosity of PET polymers at 280°C, determined in contraction flow from Binding's analysis.

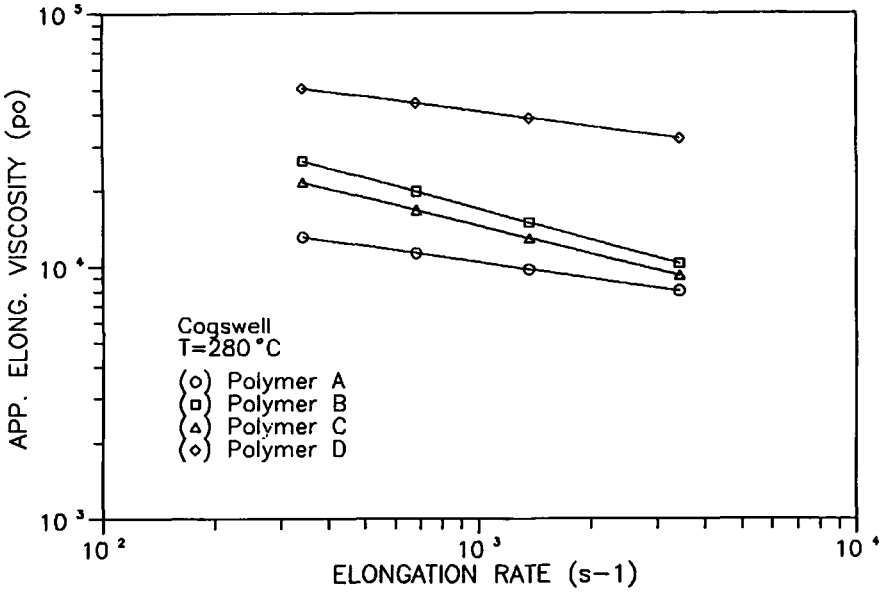

Figure 7 Apparent elongation viscosity of PET polymers at 280°C, determined in contraction flow from Cogswell's analysis.

with varying levels of complexity and therefore differing lifetimes. When the polymers are subjected to a stretching flow, the molecules may or may not have time to become untangled, and therefore they will present different responses in an orienting field. The strain thickening region corresponds to the elastic deformation of the network, whereas the strain thinning behavior is the result of a decrease

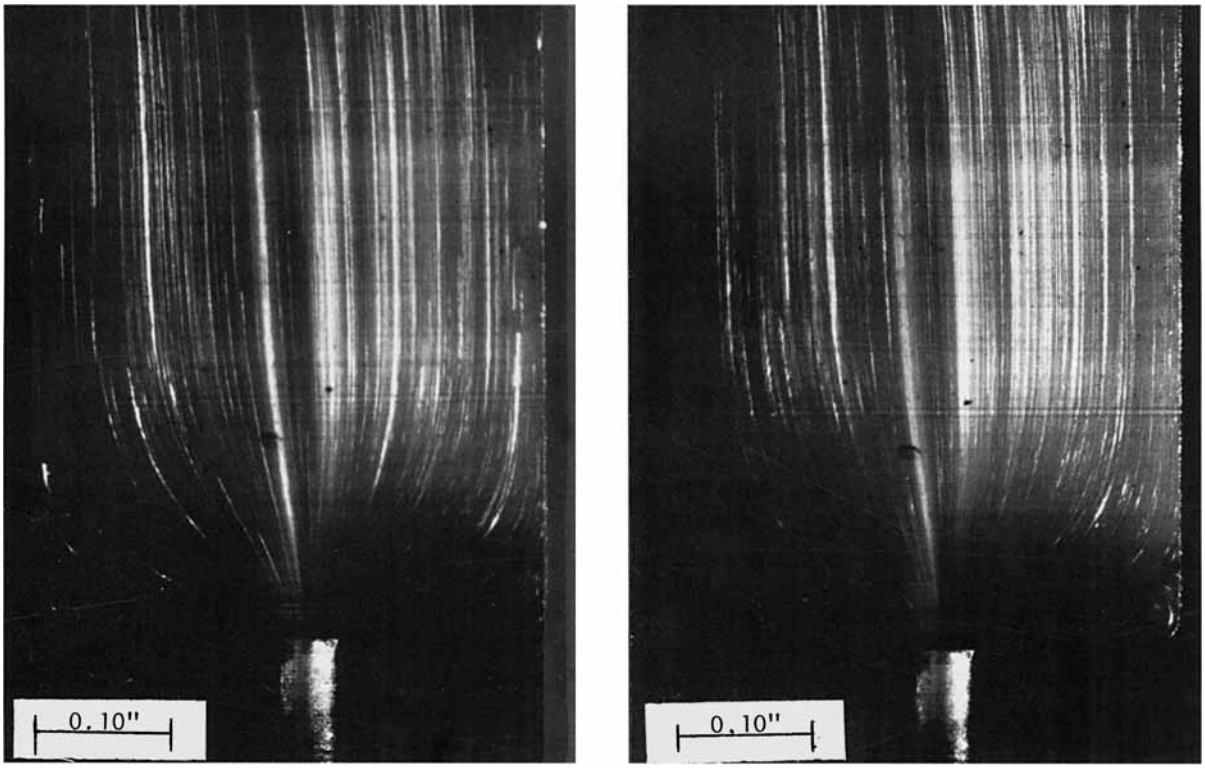

Figure 8 Convergence profile of polymer A in an axisymmetric contraction flow at 280°C. Contraction ratio 9.35 : 1; shear rate 534 s^{-1} (left), 1603 s^{-1} (right).

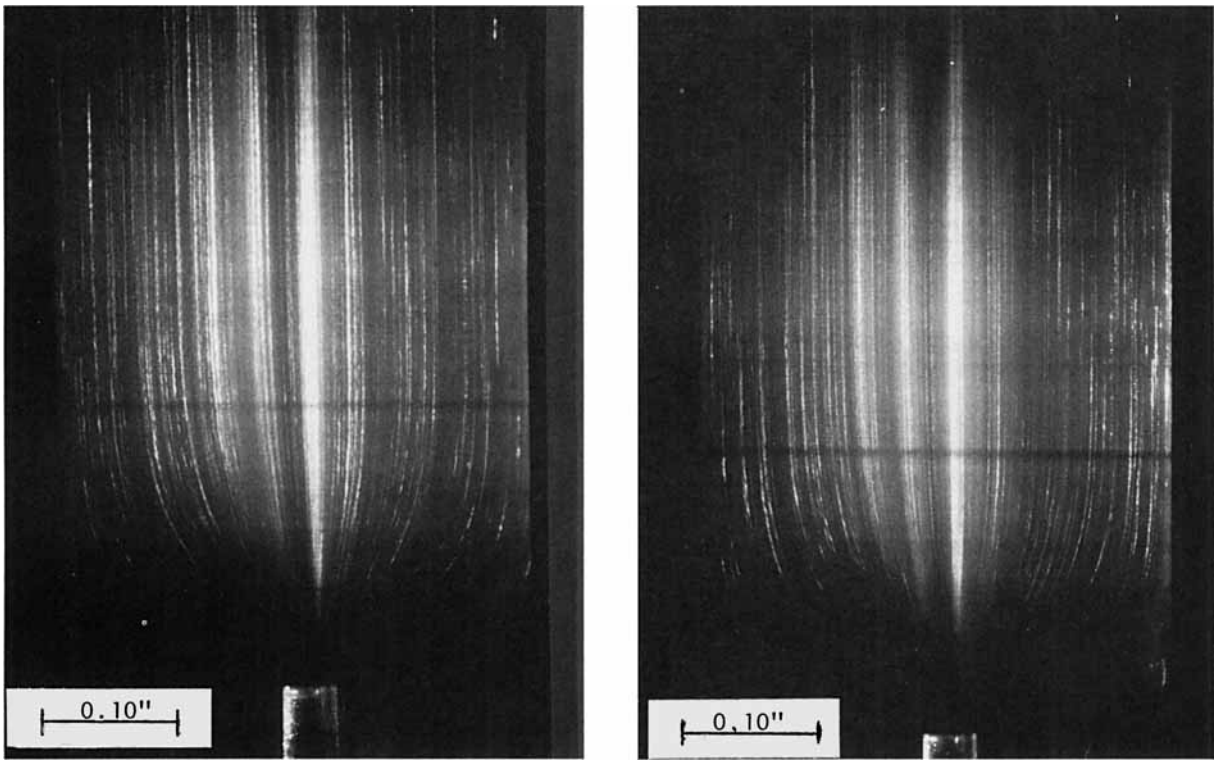

Figure 9 Convergence profile of polymer B in an axisymmetric contraction flow at 280°C. Contraction ratio 9.35 : 1; shear rate 534 s^{-1} (left), 1603 s^{-1} (right).

of the number of network junctions due to untanglement.[13] These effects are not observed in shear flow since the molecules are alternately under extension and compression and no overall orientation results. The effects of chain branching[14] and molecular weight distribution[15] have been successfully explained by this model. They also explain the striking differences in extensional flow presented by polymers that show similar shear behavior.[16]

The tension thinning behavior observed in this study for the four linear PET polymers with different IV are consistent with the data reported by White et al.[11] It is not possible with the present experimental apparatus to confirm the strain thickening behavior at low strain rates. However, this will not compromise the present analysis due to the primary interest in the strain rate range occurring in the threadline in the high-speed spinning process. In this range of strain rate near 10^3 s^{-1}, the elongational viscosity is shown to be tension thinning.

The higher molecular weight of polymer D and consequently longer relaxation time is reflected in a higher level of both shear and elongational viscosities. Likewise, the shear and elongational viscosities of polymer A are consistent with its lower molecular weight. From Figure 3 it is possible to estimate a characteristic relaxation time from the ratio of the zero shear viscosity to the shear modulus of polymer A to be approximately equal to 1 ms. This value is of the expected order of magnitude reported in the literature.[11] The characteristic relaxation time of polymer D is expected to be five times larger than that of polymer A, which explain the large difference in the shear and elongational behavior.

Polymers B and C, which show similar shear viscosity, have distinct elongational viscosity. According to the network model, it is presumed that polymer B, which shows larger elongational viscosity than polymer C, contains a larger fraction of long relaxation time molecules than does polymer C. As will be discussed further in the spinning experiments, these polymers present distinct spinnability, which is reflected in the minimum denier attainable under similar spinning conditions. The ability to predict different processability between polymers, otherwise similar in shear, seems to justify the application of the contraction flow experiments, even though restrictions have been made on the absence of a true steady state.

Comparison of the Results of the Apparent Elongational Viscosity of PET Polymers Obtained from Cogswell and Binding Analysis

The similar qualitative results of the Cogswell and Binding analysis can be shown to be a consequence of the same strain rate dependency of the elongational viscosity when the entrance pressure drop can be represented by a power law model with the shear rate. The results in Figures 4 and 5 show that a straight line is obtained in plots of log P_0 versus log shear rate, and therefore,

$$P_0 \sim \epsilon_s^m$$

From Binding's analysis, Eq. (3), it can be seen that

$$m = \frac{t(1+n)}{1+t}$$

and therefore $t = m/(1 + n - m)$, where $\mu_E \sim \epsilon_E^{t-1}$.

From Cogswell's analysis, Eqs. (1) and (2), it can be shown that

$$\mu_E \sim \frac{P_0^2}{\epsilon_s^{n+1}} \sim \frac{P_0}{\epsilon_E} \sim \frac{\epsilon_s^m}{\epsilon_E}$$

Since $\epsilon_E \sim \epsilon_s^{n+1}/P_0 \sim \epsilon_s^{1+n-m}$

$$\mu_E \sim \epsilon_E^{m/(1+n-m)-1} \sim \epsilon_E^{t-1}$$

Therefore, the flow behavior index in extensional flow is shown to be the same in both treatments. This was also observed by Tremblay[17] in the study of polyethylene flow.

The difference in the magnitude of the elongational viscosity, calculated from the two methods, is reflected in the values of Trouton ratio. Since the elongational viscosity and shear viscosity depend on the strain rate and shear rate, respectively, there is a need to define unambiguously the deformation rate at which the viscosities are to be defined. Following Jones et al.,[18] the Trouton ratio (TR) is defined as follows:

$$\mathrm{TR} = \mu_E(\epsilon)/\mu_S(\sqrt{3}\epsilon)$$

where ϵ is the reference deformation rate.

Table II summarizes the calculated values of TR from the Cogswell and Binding analysis at two values of deformation rates and at the temperature of 280°C.

Table II Comparison of TR Calculated from Binding and Cogswell Analysis at 280°C

		Strain Rate (s^{-1})	
Sample	Method	683	1367
A	Cogswell	7.4	7.4
	Binding	4.6	4.4
B	Cogswell	9.4	8.6
	Binding	5.3	4.8
C	Cogswell	8.2	7.5
	Binding	4.7	4.3
D	Cogswell	8.3	10.1
	Binding	5.3	6.1

The results in Table II indicate that the TR is almost unchanged with the deformation rate. Polymer D tends to present larger values of TR. The largest difference is due to the method employed, with the results from the Binding analysis closer to the value of 3 for a newtonian, inelastic polymer. The difference in the magnitude of the calculated elongational viscosity from the Cogswell analysis may also be attributed to the lack of taking into account the effect of the contraction ratio on the value of entrance pressure drop, as does the Binding analysis. Even though this fact alone may not explain the differences observed, experimental results show an increase of the entrance pressure drop when the contraction ratio R_1/R_0 increases.[19] The curves show, however, the same dependency on the shear rate, which supports the fact that the rate dependency of the elongational viscosity remain unchanged with varying contraction ratios.

Flow Patterns of PET Polymer Melts in a Flat Entry Die

The results of the flow visualization experiments, where no vortex growth was observed, are consistent with the calculations of the vortex length using the Binding analysis.[2] According to Binding's analysis,[2] the dimensionless vortex length $L_V/2R_1$ can be calculated by

$$\frac{L_V}{2R_1} = \frac{1+t}{2(2t-3n-1)(1+n)} \times \left[\frac{Lt(3n+1)n^t I_{nt}}{K}\right]^{1/(1+t)} (\epsilon_s)_{R_0}^{(t-n)/(1+t)} \times \alpha(1-\alpha^{(2t-3n-1)/(1+t)}) \quad (4)$$

where the symbols are the same as those used in Eq. (3).

Table III presents the calculated dimensionless vortex length $L_V/2R_1$ at 280°C and shows no vortex enhancement with an increase in deformation rate.

Vortex growth has been described as a stress relief mechanism.[20] This happens most often with a pseudoplastic polymer that shows a strain thickening behavior as in low-density polyethylene melts. This same reasoning can be applied to explain the absence of vortex growth for the present case of strain thinning polymers, where the elongational viscosity decreases as slowly as the shear viscosity with an increase in the deformation rate. Therefore no stress buildup is observed. This is also reflected in the unchanged TR with changes in deformation rate.

Significance of the Apparent Elongational Viscosity on the Melt-Spinning Behavior

The observed tension thinning behavior in the range of deformation rates used in this study is not in conflict with the reported necking phenomena in high-speed spinning. During necking the elongational rate passes through a maximum while the spinline tension increases monotonically. Therefore the spinline viscosity drops during necking, and it has been assumed that this drop is not related to a possible increase of the spinline temperature, but no definite explanation has been given at this time.[21,22] Ziabicki[23] shows that an S-shaped spinline velocity profile, characteristic of a necking phenomena, is observed with a strain thinning polymer. However, he argues that an additional source of viscosity gradient due to the stress-induced crystallization is necessary for explaining the necking phenomena. This requires further study that is complicated by the fact that neither the results of the elongational viscosity obtained in contraction flow nor the deformations in the threadline represent equilibrium conditions in the Lagrangian sense, since the extension rate varies along the capillary as well as in the threadline.

Table III Dimensionless Vortex Length as a Function of the Strain Rate. Temperature = 280°C.

Strain Rate (s^{-1})	Polymer	
	A	B
342	0.940	1.505
683	0.998	1.423
1367	0.944	1.370
3417	0.953	1.242

According to Laun and Schuch,[16] polymers with lower elongational viscosity, but similar shear viscosity, generate lower draw-down tension and therefore can be extended at higher speeds before breakage of the extrudate happens. For the case of the fine denier melt spinning, similar results should apply since the minimum denier limit is determined by the balance between the spinline strength and the increasing spinline stress with decreasing denier. The lower elongational viscosity may contribute to a lower spinline stress and therefore to a lower limit of the minimum denier. Figure 10 shows the preliminary results of the minimum attainable denier at different take-up speeds for the three low IV polymers. At take-up speeds below 3000 m/min, the values of the minimum denier are very low, and the observed differences among the polymers are mainly due to the conditions of polymer flow distribution in the pack. The flow conditions inside the pack are critical at the low take-up speed range due to the very small throughputs involved in our experimental apparatus. However, at speeds above 4000 m/min, and particularly at 5000 m/min, polymer with lower apparent elongational viscosity level allows spinning of finer denier fibers, thus confirming the role of the elongational properties of the polymer melt on its spinnability. This point will be discussed in more detail in a subsequent report along with the results of the spinning experiments.

CONCLUSIONS

The rheological characterization of four PET polymers in shear as well as in elongational flow has been performed.

The elongational viscosity parameters have been determined in contraction flow experiments following the methods proposed by Cogswell and Binding. The results obtained for the low and high IV polymers at 280°C show a tension thinning behavior in the strain rate range of 300–3000 s^{-1}. These results were explained on the basis of the network model.

A comparison of the methods of Cogswell and Binding shows that the elongational viscosity has the same strain rate dependency in both methods. However, the magnitude of the elongational viscosity are different, in part due to Cogswell's analysis failure to include the effect of the contraction ratio.

The values of the Trouton ratio were unchanged with the deformation rate, which can explain the absence of vortex growth. These observations are also consistent with the flow visualization experiments.

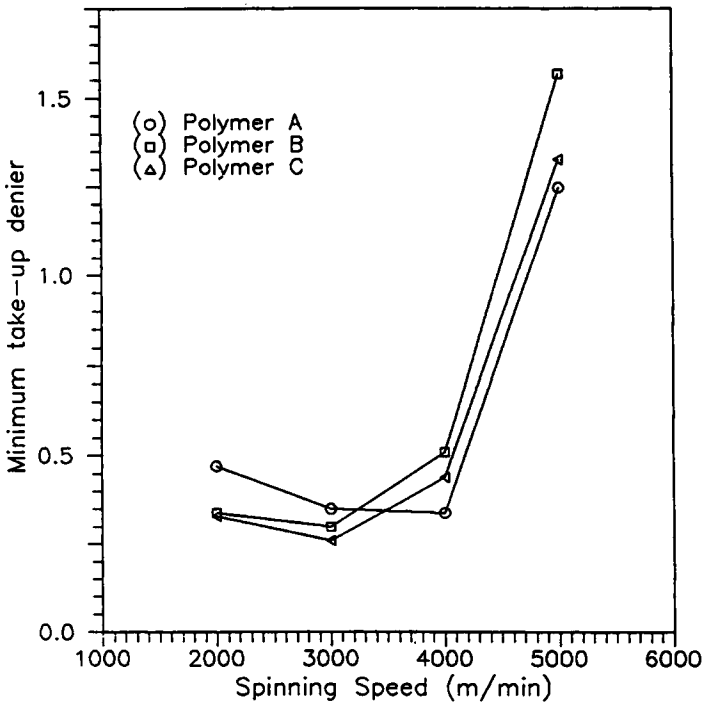

Figure 10 Minimum as-spun denier as a function of take-up speed and different PET polymers. T = 295°C, sp. 14 × 0.23 mm ($L = 2.5D$), L = 2.6 m, without quench/heating.

Despite the caution that one should take in interpreting the results of the contraction flow experiments, due to the absence of a true steady state and simplifications involved in the derivations, the use of the apparent elongational viscosity values seems justifiable in view of their ability to distinguish polymers of similar shear behavior. Their ability to predict processability of the polymers, in particular the minimum denier attainable in the melt-spinning process, is the main motivation of this research.

The authors wish to acknowledge the financial support received from Rhodia S.A.

REFERENCES

1. F. N. Cogswell, *Polym. Eng. Sci.*, **12**(1), 64–73 (1972).
2. D. M. Binding, *J. Non Newtonian Fluid Mechanics*, **27**, 173–189 (1988).
3. D. M. Binding and K. Walters, *J. Non Newtonian Fluid Mechanics*, **30**, 233–250 (1988).
4. S. Berkowitz, *J. Appl. Polym. Sci.*, **29**, 4353–4361 (1984).
5. E. B. Bagley, *J. Appl. Phys.*, **28**(5), 624–627 (1957).
6. R. N. Shroff, L. V. Cancio, and M. Shida, *Trans. Soc. Rheology*, **21**(3), 429–446 (1977).
7. D. H. Crater, Ph.D. Thesis, Fiber and Polymer Science, North Carolina State University, Raleigh, 1983.
8. W. Philippoff and F. H. Gaskins, *Trans. Soc. Rheology*, **II**, 263–284 (1958).
9. E. B. Bagley, *Trans. Soc. Rheology*, **V**, 355–368 (1961).
10. J. W. Hill and J. A. Cuculo, *J. Appl. Polym. Sci. Appl. Polym. Symp.*, **33**, 3–29 (1978).
11. J. L. White and H. Yamane, *Pure Appl. Chem.*, **57**(10), 1441–1452 (1985).
12. R. B. Bird, C. F. Curtiss, R. C. Armstrong, and O. Hassager, *Dynamics of Polymeric Liquids*, Vol. 2, 2nd, ed., Wiley, New York, 1987.
13. J. Fergurson, N. E. Hudson, B. C. H. Warren, and A. Tomatarian, *Nature*, **325**, 6101, 234–236 (1987).
14. F. N. Cogswell, *Polymer Melt Rheology*, Wiley, New York, 1981.
15. H. Munstedt, *J. Rheology*, **24**(6), 847–867 (1980).
16. H. M. Laun and H. Schuch, *J. Rheology*, **33**(1), 119–175 (1989).
17. B. Tremblay, *J. Non Newtonian Fluid Mechanics*, **33**, 137–164 (1989).
18. D. M. Jones, K. Walters, and P. R. Williams, *Rheological Acta*, **26**, 20–30 (1987).
19. C. D. Han, *AIChe J.*, **17**(6), 1480–1485 (1971).
20. J. L. White and A. Kondo, *J. Non Newtonian Fluid Mechanics*, **3**, 41–64 (1977/1978).
21. K. Fujimoto, K. Iohara, S. Owaki, and Y. Murase, *Sen-I Gakkaishi*, **44**(2), 53–58 (1988).
22. G. Vassilatos, B. Knox, and H. Frankfort, in A. Ziabicki and H. Kawai, Eds., *High Speed Fiber Spinning*, Wiley, New York, (1985).
23. A. Ziabicki, *J. Non Newtonian Fluid Mechanics*, **30**, 141–155 (1988).

Received October 29, 1991
Accepted November 4, 1991